Controlling the strong field dynamics by a time-delayed near- and mid-infrared two-color laser field

Chengpu Liu and Takashi Nakajima*
Institute of Advanced Energy, Kyoto University, Gokasho, Uji, Kyoto 611-0011, Japan
(Received 26 June 2008; revised manuscript received 14 November 2008; published 30 December 2008)

We theoretically demonstrate that the strong field dynamics such as above-threshold ionization and high-order harmonic generation can be significantly altered by the introduction of the time-delayed two-color laser field consisting of the near-infrared and mid-infrared frequencies. Specifically we apply the idea to the one-dimensional hydrogen atom, and show that the strong field dynamics significantly depend on the time delay between the two fields, as represented, for instance, by the change of the cutoff energies of above-threshold ionization and high-order harmonic generation. It turns out, however, that the delay dependence is different for those processes. In particular, if the duration of the near-infrared pulse is as short as a few cycles, its carrier-envelope phase also plays a very important role. Our classical results for the two processes are consistent with the numerical results.

DOI: 10.1103/PhysRevA.78.063424 PACS number(s): 32.80.Rm, 42.65.Ky

I. INTRODUCTION

The interaction of an atom with an intense laser field has revealed many interesting phenomena such as above-threshold ionization (ATI) [1] and high-order harmonic generation (HHG) [2]. Since the first experimental discoveries of ATI and HHG in the late 1970s and early 1990s, respectively, those processes have been extensively investigated from both theoretical and experimental aspects [3–5].

While the goal of many studies on the ATI and HHG processes is to provide clear understanding for the processes of interest, there are also many other studies with a flavor of coherent control, the aim of which is to improve the outcome after the strong field interaction where "improve the outcome" means the enhancement of the HHG signal [6] and the extension of the HHG cutoff energy, etc. To enhance the HHG signal, for example, a two-color field consisting of the fundamental field (800 nm) and its second [7,8] or third harmonic [9] is often employed with the controlling parameters such as the relative phase and/or the intensity ratio between the two fields, and/or laser polarization. Recently dramatic enhancement of high-order harmonics is experimentally realized via mixing gases with different ionization potentials [10]. Extension of the HHG cutoff energy is more demanding, since it is essentially determined by the ponderomotive energy, which is directly connected with the photon energy and field amplitude. Nevertheless, a few ideas have been proposed. For example, a combination of the 800 nm field and the dc field is employed to extend the HHG cutoff energy [11–13]. Such schemes, however, require an extremely strong dc field, and naturally they are rather impractical for experimental realization. As an alternative, one may replace the dc field by an ac field with a sufficiently long optical period compared with the duration of the 800 nm pulse [14,15]. Namely, a two-color field consisting of the fundamental (near-infrared) field with a short pulse duration and the long wavelength (mid- or far-infrared) field can be a useful tool to control the strong field dynamics. The dynamics induced by the two-color (near-infrared plus mid-infrared) field must be certainly different from those induced by the other kind of two-color (near-infrared plus its second- and/or third-harmonic generation) field due to the completely different optical period of the additional field.

To our knowledge, however, investigation on the strong field dynamics by the two-color (near-infrared plus mid-infrared) field in terms of the time delay between them and the carrier-envelope phase (CEP) still lacks in the literature, in particular for the ATI process. Moreover, very few papers report the study on both ATI and HHG processes even for the single-color field in the long wavelength [16–20]. Note that the ATI and HHG processes are strongly related and complementary to each other, and hence studying both processes should help us to deepen the physical understandings.

The purpose of this paper is to investigate the ATI and HHG processes under the time-delayed two-color laser field consisting of the near-infrared and mid-infrared frequencies. Through the numerical solution to the one-dimensional (1D) time-dependent Schrödinger equation (TDSE), we show that the strong field dynamics significantly depend on the time delay between the two fields, as represented, for instance, by the change of the cutoff energies of ATI and HHG. The delay dependence, however, turns out to be different for those processes. Furthermore, we show that, if the duration of the near-infrared pulse is as short as a few cycles, the CEP of the near-infrared pulse also plays a very important role. We additionally perform the classical analysis to shed some light on the quantum mechanical (TDSE) results. Although we specifically present results for the 1D hydrogen atom, the underlying physics is rather clear and general, and can be applicable to other system under a different context such as Coulomb explosion of molecules and clusters [21].

II. METHOD

To study the strong field dynamics, we numerically solve the TDSE. It reads

*t-nakajima@iae.kyoto-u.ac.jp

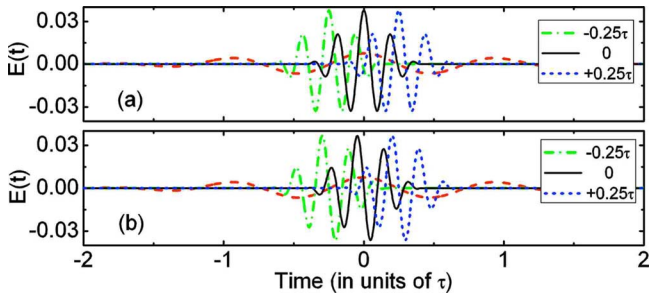

FIG. 1. (Color online) Time-delayed two-color laser field considered in this paper. Specifically we assume 4 μm and 800 nm laser fields with two-cycle (FWHM) durations ($N_{p1}=N_{p2}=2$), and the CEPs of $\Phi_1=0$, and (a) $\Phi_2=0$ and (b) $\Phi_2=0.5\pi$. The dashed curve represents the 4 μm field, and the dot-dashed, solid, and short-dashed curves represent the 800 nm laser field with delay $\Delta t=-0.25\tau$, 0, and $+0.25\tau$, respectively, where τ stands for the optical period of the 4 μm field.

$$i\frac{\partial\Psi(t)}{\partial t}=[H_0+V(t)]\Psi(t), \tag{1}$$

where $\Psi(t)$ represents the total wave function of the system, and H_0 and $V(t)$, respectively, are the field-free atomic Hamiltonian and the time-dependent interaction between the electron and the laser field. Under the electric dipole approximation, $V(t)$ is written as $V(t)=E(t)\hat{\varepsilon}\cdot\boldsymbol{r}$ with $E(t)$ being the electric field, $\hat{\varepsilon}$ the polarization vector, and $\boldsymbol{r}$ the position operator of the electron. The atomic units (a.u., $m=\hbar=e=1$) are used throughout this paper, unless otherwise mentioned. The electric field $E(t)$ is defined via the vector potential $A(t)$ as $E(t)=-\partial A(t)/\partial t$. The vector potential of the two-color field is defined as

$$\begin{aligned}A(t)&=A_1(t)+A_2(t-\Delta t)\\&=A_{10}\cos^2\left(\frac{\pi t}{2\tau_{p1}}\right)\sin(\omega_1 t+\Phi_1)\\&\quad+A_{20}\cos^2\left(\frac{\pi(t-\Delta t)}{2\tau_{p2}}\right)\sin[\omega_2(t-\Delta t)+\Phi_2].\end{aligned} \tag{2}$$

Here A_{i0}, ω_i, and $\Phi_i(i=1,2)$ are the peak amplitude of the vector potential, the central frequency, and the CEP for the field i, respectively. To save the computation time, the cosine-squared temporal field envelope is employed. The pulse duration of field i, τ_{pi}, is defined for the full width at half maximum (FWHM) as $2\pi N_{pi}/\omega_i$, where N_{pi} is the number of cycles for the FWHM. Δt is the time delay of field 2 with respect to field 1. In this paper we specifically assume that the two-color field consists of the 4 μm (field 1) and 800 nm (field 2) components. Since the 4 μm field can be produced from the 800 nm field through the difference frequency mixing, the time delay between the two fields can be precisely controlled. Figure 1(a) [Fig. 1(b)] shows the relative positions of the two laser fields for three different time delays for $\Phi_2=0$ ($\Phi_2=0.5\pi$). Note that the time delay is defined in units of the optical period of the 4 μm field τ throughout this paper.

III. ATI AND HHG SPECTRA

In the following, without a loss of generality, we employ a 1D atom [22] with a single-active-electron approximation as the screened soft-core potential model, i.e., $V(x)=-\alpha/\sqrt{1+x^2}$, where α is an adjustable parameter. For the 1D hydrogen atom, α is set to be 0.775, which yields the ground state energy of −13.6 eV [23]. Once the TDSE given in Eq. (1) has been solved using the Crank-Nicholson method, we can calculate the ATI spectra by taking a projection of the wave function, $\Psi(t)$, after the pulse onto the positive energy states, which are separately calculated by solving the "time-independent" Schrödinger equation without the laser field [17,22]. Since we use a box with a finite size, the continuum states are described as discrete (quasicontinuum) states. To increase the smoothness of the ATI spectra, we have employed a linear interpolation for the quasicontinuum energies and averaged over four consecutive points. The HHG spectra can be obtained by taking the fast Fourier transforms (FFTs) of the dipole acceleration during the time propagation.

A. ATI spectra

We now present results for the ATI spectra. The laser parameters we have chosen are $N_{p1}=2$, $I_1=2\times10^{12}$ W/cm^2, and $\Phi_1=0$ for the 4 μm field, and $N_{p2}=2$, $I_2=5\times10^{13}$ W/cm^2, and $\Phi_2=0$ for the 800 nm field, as shown in Fig. 1(a). The laser intensities have been chosen in such a way that they result in the same ponderomotive energy (3 eV) for each field. Note that we have assumed a short pulse duration for the 4 μm field for the computational reason, since, due to the use of the long wavelength field, the box size to propagate the wave function must be very large. This is particularly true for the ATI process if one wishes to obtain the ATI spectra down to the cutoff region. In the following calculations, we set the box size to be 20 000 a.u. with a spatial step of 0.1 a.u. One may have some concern about the specific choice of the CEP's, i.e., $\Phi_1=\Phi_2=0$, since the pulse durations are as short as $N_{p1}=N_{p2}=2$ for both fields. However, the effect of the CEP for the 4 μm field is effectively taken into account through the small time delay (a fraction of τ) between the two fields. Therefore without so much loss of generality we may choose the value for Φ_1 as 0. As for the 800 nm field, the CEP plays an important role as we will show later on.

First we compare the ATI spectrum by the single-color (800 nm) field with that by the two-color (4 μm+800 nm) field with zero time delay. The results are shown in Fig. 2(a). For the single-color case, we find a typical behavior for the high order ATI spectrum: As the photoelectron energy increases, we observe a clear change of the slope, which is followed by the cutoff. However, neither clear ATI peaks nor clear plateau are observed due to the short pulse duration. When the 4 μm laser field is additionally introduced with zero time delay, the plateau and accordingly the cutoff position is significantly extended. Needless to say, this is due to the combined effect of the two fields. Note that the electron ejection probability (signal intensity) around region B for the two-color case is a little bit smaller than that around region A for the single-color case.

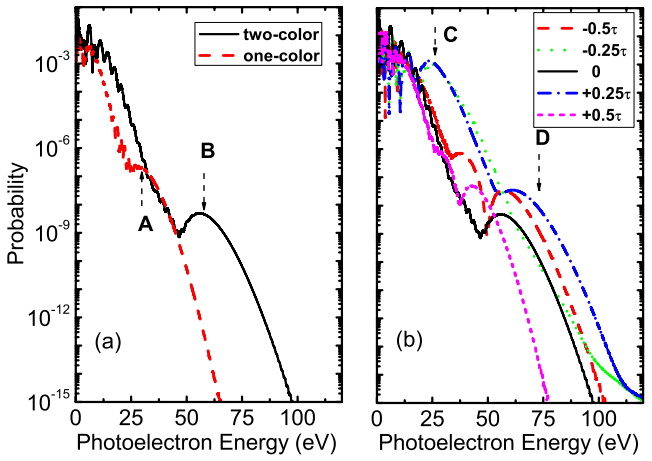

FIG. 2. (Color online) ATI spectra of 1D hydrogen atom irradiated by the single-color (800 nm) or two-color (4 μm+800 nm) laser field. (a) ATI spectra by the single-color (dashed curve) and two-color (solid curve) fields with zero time delay. (b) ATI spectra by the two-color field with different delays. The laser parameters for the 4 μm laser field are $N_{p1}=2$, $I_1=2\times10^{12}$ W/cm^2, and $\Phi_1=0$, and those for the 800 nm field are $N_{p2}=2$, $I_2=5\times10^{13}$ W/cm^2, and $\Phi_2=0$.

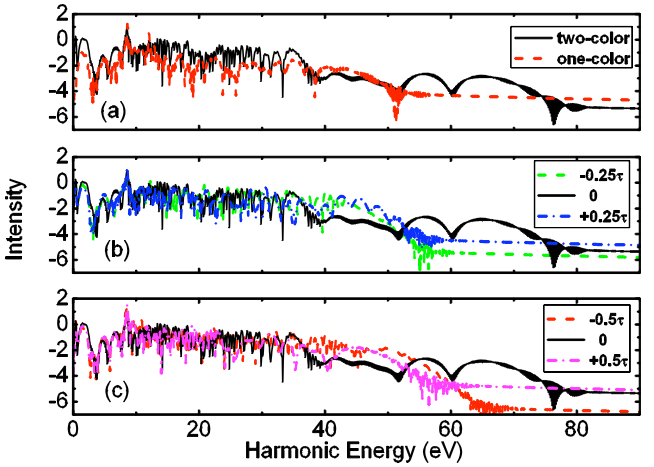

FIG. 3. (Color online) HHG spectra of 1D hydrogen atom irradiated by the single-color (800 nm) or two-color (4 μm+800 nm) laser field. (a) HHG spectra by the single-color (dashed curve) and two-color (solid curve) fields with zero time delay. (b) and (c) HHG spectra by the two-color field with different delays. The intensities are $I_1=6\times10^{12}$ W/cm^2 and $I_2=1.5\times10^{14}$ W/cm^2 with all other parameters taken to be the same with those for the ATI spectra in Fig. 2.

Now we change the time delay between the two fields. The results are shown in Fig. 2(b). The ATI spectra clearly show the delay dependence: Not only the shape of the ATI spectra but also the signal intensity are significantly altered as the time delay changes. Note, however, that the height and shape of the plateaus calculated by the 1D TDSE should not be directly compared with the experimental results or 3D TDSE results, since the electron motion is simplified in the 1D model. When the time delay is $+0.25\tau$, the plateau and cutoff shift towards the high energy side compared with the case of zero time delay. When the delay is -0.25τ, one may expect some difference in the ATI spectrum with that for the $+0.25\tau$ time delay, since the combined fields for $\pm0.25\tau$ time delays are different, as one can see from Fig. 1(a). Indeed, although the spectra in the low energy region (region C) are similar, there exists a clear difference in the high energy region (region D); that is, for the former there is no clear change of the slope. For the cases of $\pm0.5\tau$ time delays, the difference becomes larger, especially in the higher energy region. This must be entirely due to the use of the time-varying 4 μm laser field, since this should not happen if the 4 μm laser field has a constant envelope. Most importantly, the cutoff energy turns out to be the maximum when the delay is $+0.25\tau$. In Sec. III C we will make some comparisons with the classical theory.

B. HHG spectra

Having studied the ATI spectra, we now investigate the HHG spectra. We increase the intensities for both fields by a factor of 3 so that the plateaus in the HHG spectra become more visible. Hence the ponderomotive energy is 9 eV for each field now. All other parameters are taken to be the same with those for the ATI spectra in Figs. 2(a) and 2(b). Figure 3(a) shows the HHG spectra for the single-color (800 nm) field and the two-color (4 μm+800 nm) field with zero time delay. For the single-color case, we again find a typical behavior for HHG: We observe a clear plateau which is followed by a steep cutoff at the energy 43 eV, which agrees well with the well-known formula $I_p+3.17U_p$, where I_p is the ionization potential of the target atom and U_p is the ponderomotive energy. When the 4 μm field is additionally introduced with zero time delay, the plateau is significantly extended to the higher-order harmonic energy. Because of the use of only two-cycle pulses for 4 μm and 800 nm fields, the appearance of the plateau for the two-color case is neither very obvious nor flat, especially in the higher-order harmonic energy region.

Now we change the time delay between the two fields. The results are shown in Figs. 3(b) and 3(c). The time delay significantly affects the HHG spectra in terms of the positions of the cutoffs. This can be attributed to the different values of the combined field amplitudes for the different time delays. As we introduce the time delay such as $\pm0.25\tau$, $\pm0.5\tau$, and others (not shown here), the maximum harmonic energies clearly decrease compared with that for zero time delay. They are almost the same with that for the single-color case. In addition, from Figs. 3(b) and 3(c), we can ensure that, only when the delay is zero, the cutoff energy can be the maximum.

From Figs. 2 and 3, we see that the ATI and HHG processes have a common feature: Use of the two-color field significantly alters the strong field dynamics in terms of both ATI and HHG processes, and the alteration is clearly delay-dependent. It is important to note, however, that the maximum kinetic energy for HHG is at zero time delay, while it is at the time delay of $+0.25\tau$ for ATI. This difference comes from the fact that the high-order ATI and HHG processes are inherently different: The electron is eventually ejected in the former while it is eventually recombined with the core in the

latter. Therefore the optimized time delays are different for the two different processes. For a better and intuitive understanding, we perform the classical analysis in the next subsection.

C. Classical analysis

The classical theory of ATI by a single-color laser field has been given in several papers [4, 5, 17, and references therein], which can be easily extended to the two-color case. In the classical theory the electron's motion is assumed as follows: The electron is born at the origin with zero velocity at time t_0 (ionization time), and subsequently it moves under the influence of the laser field only. After some time, the electron may return to the origin and experience the recombination or elastic scattering with the core at time t_r (recombining or rescattering time). The former and the latter processes result in HHG and ATI, respectively. In this subsection we calculate the classical electron trajectory and investigate the temporal change of the electron kinetic energy in the single-color and time-delayed two-color laser fields.

By solving the Newton's equation $dr(t)/dt^2=-E(t)$, we find that the electron velocity $v(t)$ at any time after ionization can be obtained as $v(t)=A(t)-A(t_0)$ $(t>t_0)$. If the electron returns to the origin, the relation $\int_{t_0}^{t_r} dt v(t)=0$ must be always satisfied. If it recombines with the core, the electron energy is obtained by $[A(t_r)-A(t_0)]^2/2$. If it is backscattered by the core, the electron energy is obtained by $[A(T_p)-A(t_r)-v(t_r)]^2/2$. For the two-color case, $A(t)$ must be replaced by $A_1(t)+A_2(t-\Delta t)$. Note that the rescattering can take place more than once until the laser pulse is turned off at time T_p. Here we only consider the first return, since, generally speaking, the probabilities of the higher order returns should be much smaller than that of the first return. We should point out that the classical analysis we perform in this subsection is slightly different from that by Milosevic *et al.* [5], since we need to take into account the electrons flying to *both* directions along the laser polarization axis to compare with our 1D TDSE results which has no resolution on the direction of electron ejection.

It should be kept in mind that the classical analysis does not tell us with what probability the photoelectron ejection at a certain kinetic energy takes place, although it does tell us the change of electron kinetic energy as a function of ionization time with an assumption that the electrons are already in a laser field. That is, the classical analysis can take into account neither electron ejection, rescattering, nor recombining probabilities. It has some limitations. Nevertheless, such an analysis is very useful to obtain some insights for the ATI as well as HHG dynamics [4,5,17]. For example, the well known cutoff laws for HHG and ATI at $3.17U_p$ and $10U_p$ are successfully obtained for the case of a single-color field. By extending the analysis to the case of two-color field with or without time delay, we could also obtain some insights which would be helpful to understand the quantum mechanical results shown in Figs. 2 and 3.

In Figs. 4(a) and 4(b), we show the classical results for the kinetic energy of *rescattered electron* as a function of

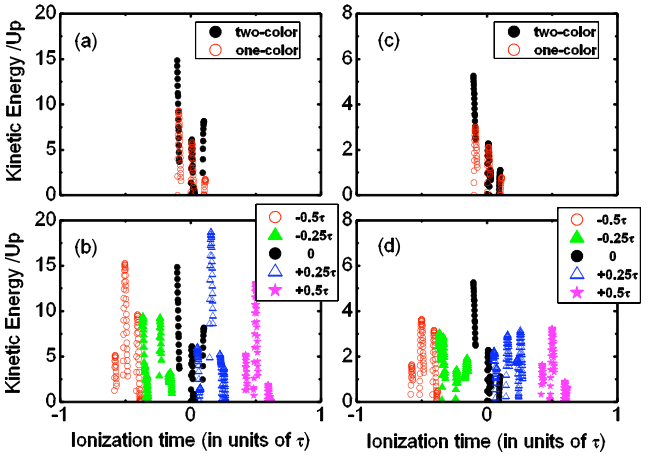

FIG. 4. (Color online) Classical results for the electron kinetic energy driven by the single-color (800 nm) or two-color (4 μm +800 nm) laser field. (a) Kinetic energy of the *rescattered* electron as a function of ionization time for the single-color (open circle) and two-color (closed circle) fields with zero time delay. (b) Similar to graph (a) but for the two-color field with different time delays. (c) Kinetic energy of the *recombining* electron as a function of ionization time for the single-color (open circle) and two-color (closed circle) fields without a time delay. (d) Similar to graph (c) but for the two-color field with different time delays. All the kinetic energy is in units of the ponderomotive energy U_p for the 800 nm laser field, which is 3 eV for ATI and 9 eV for HHG, respectively, due to the different choices of the intensities as described in the text.

ionization time t_0 with the same laser parameters employed for the calculation of ATI spectra in Fig. 2. The kinetic energy is in units of the ponderomotive energy by the 800 nm laser field only, U_p, which is 3 eV and exactly the same with the ponderomotive energy by the 4 μm laser field only. Owing to the highly nonlinear field dependence of the ionization process, only the events at the reasonably high electric field have physical significance [5]. Accordingly we focus on the events at $|E(t)| \geqslant 0.67E_{20}$ where E_{20} is the peak amplitude of the electric field of the 800 nm laser. From Fig. 4(a) we find that the maximum kinetic energies of the electron are about $9U_p$ and $15U_p$ for the single-color field and two-color field with zero time delay, respectively. That is, the maximum kinetic energy is significantly extended for the two-color case compared with the single-color case. Note that the value of $9U_p$ for the time-varying single-color field is a little bit smaller than that for the constant laser field, $10U_p$, which must be due to the pulse duration effect. By adding the contribution of the Coulomb potential, $0.538I_p$ [24], to the maximum kinetic energies of $9U_p$ $(15U_p)$ for the single-color (two-color) field, we find that the classical theory can approximately reproduce the cutoff positions of ATI in Fig. 2(a) for the single-color case [region A in Fig. 2(a)] as well as the two-color case with zero time delay [region B in Fig. 2(a)]. Figure 4(b) shows similar results with different time delays. Clearly the maximum kinetic energy of the rescattered electron under the two-color field is very sensitive to the time delay between the two fields: For the time delay of $+0.25\tau$ it takes the largest value, and for the time delay of zero and

$\pm 0.5\tau$ it takes the similar second largest values, and for the time delay of -0.25τ it takes the smallest value. Clearly the above classical analysis for ATI under the time-delayed two-color field successfully reproduces the cutoff energies for different time delays obtained by the numerical solution of 1D TDSE. However, when it comes to the height of the ATI signal which depends on the ionization as well as rescattering probabilities, there is something which cannot be explained by the classical analysis. This is the limitation of the classical analysis.

Similarly, Figs. 4(c) and 4(d) show that the maximum kinetic energy of the *recombining electron* is also very sensitive to the time delay. For the two-color case it can be significantly extended compared with the single-color case. According to Fig. 4(c), the maximum kinetic energies of the recombining electron are about $3U_p$ and $6U_p$, respectively, for the single-color field and two-color field with zero time delay. Note that the value of $3U_p$ for the time-varying single-color field is a little bit smaller than that for the constant laser field, $3.17U_p$, which is also due to the short pulse duration effect. Again, by adding the value of the ionization potential to the maximum kinetic energies of $3U_p$ $(6U_p)$ for the single-color (two-color) field shown in Fig. 4(c), we find that the classical prediction of the cutoff energy agrees rather well with the numerical results [Fig. 3(a)]. Note that the U_p for each field takes the same value, which is 9 eV. When the time delay is introduced [Fig. 4(d)], we find a reduction of the maximum kinetic energy of recombining electron. Note that this behavior for HHG is different from that for ATI. Moreover, with any finite delays (positive or negative), we see some extension of the plateau compared with the single-color case. An intuitive explanation can be that, after the birth of the electron (ionization) by the 800 nm field, the electron is further accelerated by the 4 μm field if the two-color field is employed. We would like to point out that the above findings by the classical analysis are consistent with the numerical results shown Figs. 3(b) and 3(c).

As we have shown above, the classical results agree rather well with the TDSE results presented in Figs. 2 and 3. Both ATI and HHG processes have a common feature: Use of the two-color field significantly alters the strong field dynamics and the alteration is delay-dependent. However, we notice some differences as well: (i) The maximum kinetic energy for HHG is at zero time delay, while it is at the time delays of $+0.25\tau$ for ATI. (ii) For HHG the delay dependence appears to be more symmetric compared with ATI with respect to the sign of the time delay. These differences must come from the fact that the high-order ATI and HHG processes are inherently different; that is, the electron is eventually ejected in the former while it is eventually recombined with the core in the latter.

D. Effect of the CEP

It is well known that the CEP of a few-cycle laser field has a significant effect on the interaction dynamics such as phase-dependent ionization [25]. Since we have employed $N_{p2}=2$ for the 800 nm field with $\Phi_2=0$ as shown in Fig. 1(a), we ought to consider the case with different values of

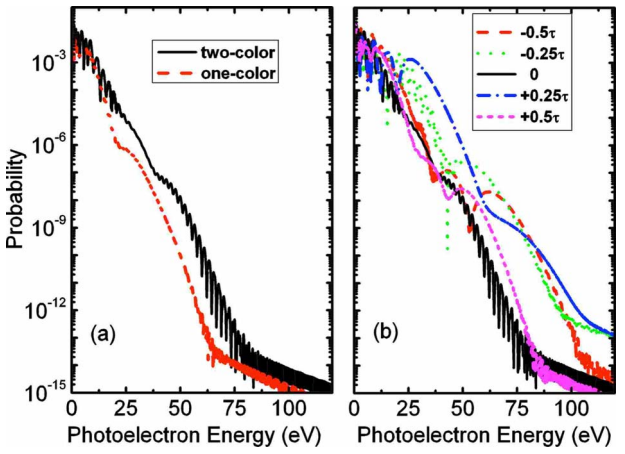

FIG. 5. (Color online) Same as those Fig. 2, but calculated for $\Phi_2=0.5\pi$.

Φ_2. Figures 5 and 6, respectively, present results for the ATI and HHG spectra with $\Phi_2=0.5\pi$ whose temporal field profile is shown in Fig. 1(b). The corresponding classical results are shown in Fig. 7. Here, similar to the reason explained in Sec. III C, we choose $|E(t)| \geqslant 0.5E_{20}$. From the comparison of Fig. 2 with Fig. 5 for ATI, and Fig. 3 with Fig. 6 for HHG, it is clear that the CEP of the 800 nm field plays an important role. First, for ATI, the maximum kinetic energies of the photoelectron and harmonic photon in the case of $\Phi_2=0.5\pi$ is slightly smaller than those for $\Phi_2=0$ with different time delays, which must be due to the different combined peak intensities employed for both cases. Second, for the case of zero time delay, the plateau (between about 37 and 50 eV) exhibits a very well-resolved beating pattern, while this is absent for the corresponding case with $\Phi_2=0$ [black curve in Fig. 2(a)]. If we refer to the classical result shown in Fig. 7(a), we can find two ionization times for the kinetic energy of $10-15U_p$. This results in the beating pattern in the ATI spectrum [black curve in Fig. 5(a)]. Moreover, the delay dependence of the cutoff energy for $\Phi_2=0.5\pi$ is also different from that for $\Phi_2=0$, although the maximum cutoff energy for $\Phi_2=0.5\pi$ is still obtained at the time delay of $+0.25\tau$. Finally for HHG, a similar conclusion can be drawn. Similar to the

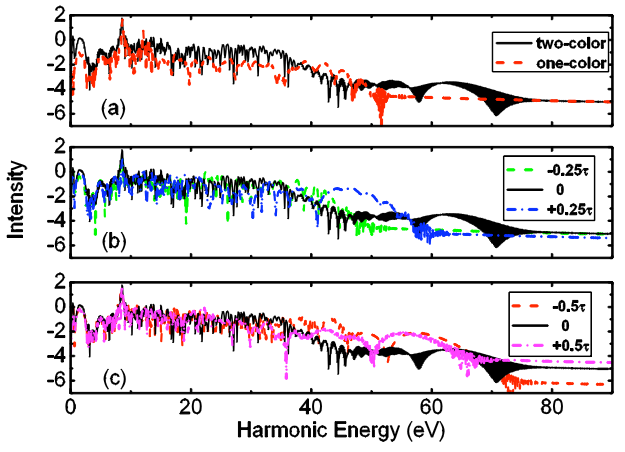

FIG. 6. (Color online) Same as those in Fig. 3, but calculated for $\Phi_2=0.5\pi$.

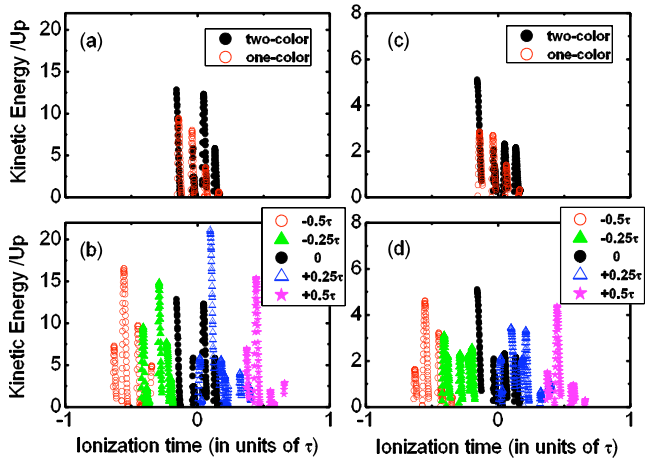

FIG. 7. (Color online) Same as those in Fig. 4, but calculated for $\Phi_2=0.5\pi$.

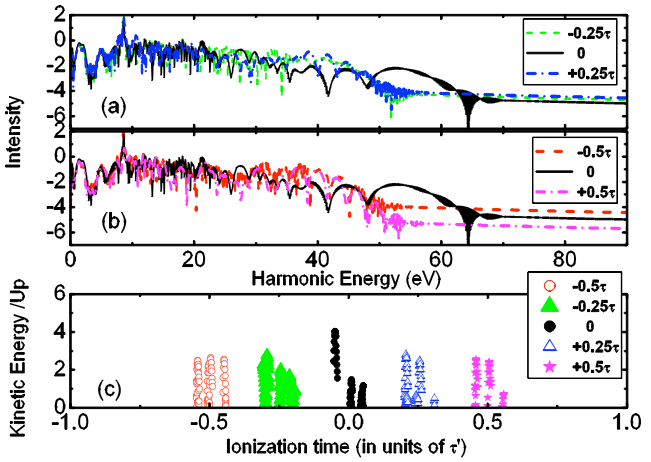

FIG. 8. (Color online) (a) and (b) HHG spectra of 1D hydrogen atom irradiated by the two-color (3.3 μm+800 nm) laser field with different delays. (c) Kinetic energy of the *recombining* electron as a function of ionization time for the two-color (3.3 μm+800 nm) field with different time delays. The laser parameters for the 3.3 μm laser field are $N_{p1}=2$, $I_1=8.8\times10^{12}$ W/cm^2, and $\Phi_1=0$, and those for the 800 nm field are $N_{p2}=2$, $I_2=1.5\times10^{14}$ W/cm^2, and $\Phi_2=0$. The kinetic energy is in units of the ponderomotive energy U_p (9 eV). τ' stands for the optical period of the 3.3 μm field.

case of $\Phi_2=0$, some features we observe in the TDSE results (Figs. 5 and 6) can be found in the classical results shown in Fig. 7. We should bear in mind that the CEP effect for the 4 μm field is only approximately taken into account through the time delay in our specific case, because we have assumed a rather short pulse duration for the 4 μm field. If the pulse duration of the 4 μm field were longer, the approximate correspondence between the CEP of the 4 μm field and the time delay would become rigorous.

In order to show that our findings are rather general, we have carried out two additional calculations. In the first calculations we have employed a different wavelength for the mid-infrared field, 3.3 μm, which is not exactly an integer multiple of 800 nm. As before, the intensity of the 3.3 μm is chosen such that the ponderomotive energies are the same for both fields. The results are shown in Fig. 8. As Fig. 8 clearly shows, the HHG cutoff energies are still sensitive to the time delay, and moreover, they agree well with the classical results. In the second calculations, we have employed a *multicycle pulse* ($N_{p2}=4$) for the 800 nm field combined with the 4 μm field (results are not shown here). As we expected, the CEP of the 800 nm field with a longer pulse duration plays a lesser role compared with the two-cycle pulse ($N_{p2}=2$) studied in this paper. It is, however, interesting to note that the effect of the time delay is still there regardless of the longer pulse duration of the 800 nm field, which is rather favorable for the experimental realization.

Thus we have confirmed that the strong field dynamics under the two-color (near-infrared and mid-infrared) laser field can be controlled through the time delay, and if the pulse duration is as short as a few cycles the CEP can also serve as a control parameter.

IV. CONCLUSIONS

In conclusion we have theoretically studied the strong field dynamics for the one-dimensional hydrogen atom under the combination of the time-delayed near-infrared and mid-infrared fields. The role of the mid-infrared field is to induce the quasistatic offset of the electric field amplitude during the interaction of the near-infrared field with target atoms. We have carried out the specific study for the 1D hydrogen atom under the influence of the 4 μm and 800 nm laser fields, and found that the time delay between the two fields plays a very important role in the strong field dynamics such as ATI and HHG. Since the pulse duration employed in this work is a few-cycle, we have also found additional but strong effects of the CEP.

One of the most eminent phenomena we have found is a change of the cutoff energies for both ATI and HHG. However, the delay dependence of the cutoff energies is different for ATI and HHG, since their dynamics are inherently different: The electron is eventually ejected in the former while it is eventually recombined with the core in the latter. Through the classical analysis for both processes, we have confirmed our conclusions. Although we have also found that the height and shape of plateaus strongly depend on the time delay and the CEP, we cannot say anything quantitative to compare with experiments, since our results presented in this paper are based on the one-dimensional calculations.

As a last remark, we note that the strong field dynamics of molecules and clusters will also be significantly altered under the two-color field, which is out of the scope of this work.

ACKNOWLEDGMENTS

T.N. is grateful to B. B. Wang for useful discussions. C.L. acknowledges financial support from the Japan Society for the Promotion of Sciences (JSPS) and the hospitality at Kyoto University during his stay. The work by T.N. was supported by a Grant-in-Aid for scientific research from the Ministry of Education and Science of Japan.

[1] P. Agostini, F. Fabre, G. Mainfray, G. Petite, and N. K. Rahman, Phys. Rev. Lett. **42**, 1127 (1979).
[2] A. L'Huillier and Ph. Balcou, Phys. Rev. Lett. **70**, 774 (1993).
[3] P. Salières, A. L'Huillier, Ph. Antoine, and M. Lewenstein, Adv. At., Mol., Opt. Phys. **41**, 83 (1999).
[4] W. Becker, F. Grasbon, R. Kopold, D. B. Milošević, G. G. Paulus, and H. Walther, Adv. At., Mol., Opt. Phys. **48**, 35 (2002).
[5] D. B. Milošević, G. G. Paulus, D. Bauer, and W. Becker, J. Phys. B **39**, R203 (2006).
[6] C. Winterfeldt, C. Spielmann, and G. Gerber, Rev. Mod. Phys. **80**, 117 (2008).
[7] H. Eichmann, A. Egbert, S. Nolte, C. Momma, B. Wellegehausen, W. Becker, S. Long, and J. K. McIver, Phys. Rev. A **51**, R3414 (1995).
[8] I. J. Kim, C. M. Kim, H. T. Kim, G. H. Lee, Y. S. Lee, J. Y. Park, D. J. Cho, and C. H. Nam, Phys. Rev. Lett. **94**, 243901 (2005).
[9] S. Watanabe, K. Kondo, Y. Nabekawa, A. Sagisaka, and Y. Kobayashi, Phys. Rev. Lett. **73**, 2692 (1994).
[10] E. J. Takahashi, T. Kanai, K. L. Ishikawa, Y. Nabekawa, and K. Midorikawa, Phys. Rev. Lett. **99**, 053904 (2007).
[11] M. Q. Bao and A. F. Starace, Phys. Rev. A **53**, R3723 (1996).
[12] A. Lohr, W. Becker, and M. Kleber, Laser Phys. **7**, 615 (1997).
[13] B. B. Wang, X. F. Li, and P. M. Fu, J. Phys. B **31**, 1961 (1998).
[14] B. Borca, A. V. Flegel, M. V. Frolov, N. L. Manakov, D. B. Miloševic, and A. F. Starace, Phys. Rev. Lett. **85**, 732 (2000).
[15] S. Odžak and D. B. Miloševic, Phys. Rev. A **72**, 033407 (2005).
[16] J. Tate, T. Auguste, H. G. Muller, P. Salières, P. Agostini, and L. F. DiMauro, Phys. Rev. Lett. **98**, 013901 (2007).
[17] Chengpu Liu, Takashi Nakajima, Tetsuo Sakka, and Hideaki Ohgaki, Phys. Rev. A **77**, 043411 (2008).
[18] P. Colosimo, G. Doumy, C. I. Blaga, J. Wheeler, C. Hauri, F. Catoire, J. Tate, R. Chirla, A. M. March, G. G. Paulus, H. G. Muller, P. Agostini, and L. F. DiMauro, Nat. Phys. **4**, 386 (2008).
[19] K. Schiessl, K. L. Ishikawa, E. Persson, and J. Burgdörfer, Phys. Rev. Lett. **99**, 253903 (2007).
[20] M. V. Frolov, N. L. Manakov, and A. F. Starace, Phys. Rev. Lett. **100**, 173001 (2008).
[21] K. Yamanouchi, Science **295**, 1659 (2002).
[22] J. Javanainen, J. H. Eberly, and Q. Su, Phys. Rev. A **38**, 3430 (1988).
[23] X. M. Zhang, J. T. Zhang, L. H. Bai, Q. H. Gong, and Z. Z. Xu, Opt. Express **13**, 8708 (2005).
[24] M. Busuladžić, A. Gazibegović-Busuladžić, and D. B. Milošević, Laser Phys. **16**, 289 (2006).
[25] G. G. Paulus, F. Grasbon, H. Walther, P. Villoresi, M. Nisoli, S. Stagira, E. Priori, and S. De Silvestri, Nature (London) **414**, 182 (2001).